General Organization of Protein in HeLa 40S Nuclear Ribonucleoprotein Particles

LEONARD LOTHSTEIN, HARTWIG P. ARENSTORF, SU-YUN CHUNG, BARBARA W. WALKER, JOHN C. WOOLEY, and WALLACE M. LESTOURGEON

Department of Molecular Biology, Vanderbilt University, Nashville, Tennessee 37235. Dr. Lothstein's present address is Department of Molecular Pharmacology, Albert Einstein College of Medicine, Bronx, New York 10461; Dr. Chung's and Dr. Walker's is National Institutes of Health, Bethesda, Maryland 20205; Dr. Wooley's is National Science Foundation, Washington, D. C. 20550.

ABSTRACT The majority of the protein mass of HeLa 40S heterogeneous nuclear ribonucleoprotein monoparticles is composed of multiple copies of six proteins that resolve in SDS gels as three groups of doublet bands (A1, A2; B1, B2; and C1, C2) (Beyer, A. L., M. E. Christensen, B. W. Walker, and W. M. LeStourgeon. 1977. *Cell.* 11: 127–138). We report here that when 40S monoparticles are exposed briefly to ribonuclease, proteins A1, C1, and C2 are solubilized coincidentally with the loss of most premessenger RNA sequences. The remaining proteins exist as tetramers of $(A2)_3(B1)$ or pentamers of $(A2)_3(B1)(B2)$. The tetramers may reassociate in highly specific ways to form either of two different structures. In 0.1 M salt approximately 12 tetramers (derived from three or four monoparticles) reassemble to form highly regular structures, which may possess dodecahedral symmetry. These structures sediment at 43S, are 20–22 nm in width, and have a mass near 2.3 million. These structures possess 450–500 bases of slowly labeled RNA, which migrates in gels as fragments 200–220 bases in length. In 9 mM salt the tetramers reassociate to form 2.0 M salt-insoluble helical filaments of indeterminant length with a pitch near 60 nm and diameter near 18 nm. If 40S monoparticles are treated briefly with nuclease-free proteases, the same proteins solubilized by nuclease (A1, C1, and C2) are preferentially cleaved. This protein cleavage is associated with the dissociation of most of the heterogeneous nuclear RNA. Proteins A2 and B1 again reassemble to form uniform, globular particles, but these sediment slightly slower than intact monoparticles. These findings indicate that proteins A1, C1, and C2 and most of the premessenger sequences occupy a peripheral position in intact monoparticles and that their homotypic and heterotypic associations are dependent on protein–RNA interactions. Protein cross-linking studies demonstrate that trimers of A1, A2, and C1 exist as the most easily stabilized homotypic association in 40S particles. This supports the 3:1 ratio (via densitometry) of the A and C proteins to the B proteins and indicates that 40S monoparticles are composed of three or four repeating units, each containing 3(A1),3(A2),1(B1),1(B2),3(C1), and 1(C2).

When isolated nuclei from mammalian cells are disrupted briefly with ultrasound (1–3) or extracted with low ionic strength buffers (4, 5), the majority of the premessenger RNA sequences (heterogeneous nuclear [hn] RNA)[1] are recovered in 20–25-nm 40S ribonucleoprotein complexes or monoparticles (1–13). Along with hnRNA, these monoparticles are primarily composed of multiple copies of six nucleus-specific polypeptides that migrate in SDS polyacrylamide gels as three groups of doublet bands (A1,A2; B1,B2, and C1,C2) with

[1] *Abbreviations used in this paper:* CuP, $(orthophenanthroline)_2Cu(II)$ complex; DTBP, 3,3′-dimethyl dithiobispropionimidate dihydrochloride; hnRNA, heterogeneous nuclear RNA; hnRNP, heterogeneous nuclear ribonucleoprotein; NRS, nuclease-resistant structure; OD, optical density.

THE JOURNAL OF CELL BIOLOGY · VOLUME 100 MAY 1985 1570–1581

molecular weights of 32,000, 34,000, 36,000, 37,000, 42,000, and 44,000, respectively (2, 5, 8–12). The 40S complexes isolated from sucrose gradients show the same ultrastructural morphology as the particles that are observed bound to nascent transcripts in gently spread chromatin (13). In spreads (at alkaline pH) of *Drosophila* embryo chromatin, particles perhaps analogous to 40S heterogeneous nuclear ribonucleoprotein (hnRNP), are observed bound to nascent transcripts at sequence-specific sites (14, 15). These particles (sometimes separated by distances as great as 23 kilobases along a single transcript) aggregate, creating loops of RNA. This event is followed by loop excision (15). These findings and others reviewed elsewhere (16–18) continue to indicate that monoparticles may function in the events of hnRNA processing.

Several efforts to obtain information on the composition and organization of protein and hnRNA in hnRNP complexes have utilized various ribonuclease digestion protocols. Early observations indicated that large hnRNP complexes (polyparticles) are converted to monoparticles by very mild nuclease activity (4, 5). Extensive digestion of monoparticles with micrococcal nuclease causes the complete dissociation of monoparticles, suggesting that protein–RNA interactions play an important role in particle structure (5, 9, 10). This is further supported by ultraviolet cross-linking studies that indicate that the major particle proteins are in contact with RNA (10, 19–21). Several groups have observed that most of the rapidly labeled premessenger sequences associated with monoparticles are easily cleaved with nuclease (8, 22), prompting some to conclude that these sequences are peripherally positioned on monoparticles (8). A second interpretation of these results was made by Stevenin et al. (23) who concluded that two types of hnRNP particles exist (α- and β-particles). Both particles were believed to co-sediment in sucrose gradients and to have the same buoyant density. The α-particles (containing a small subset of the hnRNP proteins) were defined by their resistance to nuclease; the β-particles (more heterogeneous in protein composition) were defined as those especially labile to nuclease action. These investigators concluded in a later report that α-particles do not exist prior to nuclease action, but are an artifactual rearrangement product produced by nuclease activity (24). This logic was based on the observation that the particles remaining after brief nuclease digestion sediment slightly faster in gradients and appear larger in electron micrographs than intact monoparticles.

We report here that proteins A2 and B1 are positioned internally in intact 40S hnRNP particles. Protein A2 exists as a homotypic trimer associated with B1 and B2 to form $(A2)_3(B1)$ tetramers and $(A2)_3(B1)(B2)$ pentamers. Proteins A1, C1, and C2 are positioned peripherally and, like protein A2, proteins A1 and C1 also exist as homotypic trimers in monoparticles. When the peripheral proteins dissociate after either limited ribonuclease or protease digestion, the internal $(A2)_3(B1)$ tetramers reassemble to form either of two highly ordered structures. Under conditions of limited nuclease activity approximately 12 tetramers (derived from three or four monoparticles) reassemble to form homogeneous 43S particles, which appear in electron micrographs as regular six-sided structures. If these nuclease-resistant structures (NRS) are equilibrated in low salt, the tetramers reassociate to form very long helical filaments whose structure is not dependent on the presence of RNA and is not dissociated at 2.0 M NaCl. Filaments possibly analogous to those described here have been observed in nuclease digests of oocyte hnRNP and were assumed to be elements of a nuclear matrix (25). The findings reported here allow the mass, protein copy number, stoichiometry, and general arrangement of the major proteins in intact particles to be approximated.

MATERIALS AND METHODS

Cell Growth, Fractionation, and Gel Electrophoresis: HeLa cells were grown in suspension culture in minimal essential medium supplemented with 5% calf serum and harvested in log-phase growth at an optimum density of $4–5 \times 10^5$ cells/ml. Nuclei were isolated in NHS buffer (20 mM Tris-HCl, pH 7.2, 1.0 mM $MgCl_2$, 0.02% Triton X-100) as described previously (5). Nuclear purity was monitored by phase-contrast microscopy. Monomer hnRNP particles were released from nuclei as previously described either by passive diffusion (5, 9) or by sonic disruption (2, 3). In some cases the latter procedure was modified to include incubation of the disrupted nuclei at 37°C for 10 min prior to the removal of membrane fragments, nucleoli, chromatin and intact nuclei by centrifugation. The hnRNP particles were further purified by sedimentation through 15–30% sucrose gradients (Schwarz-Mann Div., Becton, Dickson & Co., Orangeburg, NY; ribonuclease-free) at 4°C in STM buffer (90 mM NaCl, 1.0 mM $MgCl_2$, 10 mM Tris-HCl, pH 8.0) for 16 h at 25,000 rpm in an SW-27 rotor (Beckman Instruments, Inc., Fullerton, CA). Protein was analyzed by SDS-polyacrylamide slab gel electrophoresis as described previously (26). RNA was extracted from various preparations using 1 vol each of redistilled phenol, pH 8.0, and chloroform/isoamyl alcohol (24:1), followed by the addition of potassium acetate to 0.3 M and precipitation in 2.5 vol of 95% ethanol overnight at −20°C. Electrophoresis was performed in 4.0% polyacrylamide containing 4.0 mM Tris-acetate, pH 8.1, at 110 V for 2.5 h. The gels were equilibrated in ethidium bromide 0.05 μg/ml in 1.0 mM Na2-EDTA, pH 8.0, and the RNA was visualized by ultraviolet illumination.

Electron Microscopy: Both unfixed samples and samples fixed with 0.1% glutaraldehyde were used to determine the number of 40S monoparticles that give rise to a 43S NRS. For particle counting by the adsorption method, grids were floated on a 20-μl drop of sample (previously dialyzed against STM buffer) for 60 s, then on three successive drops of 2% ammonium acetate for 5 s each, then on 1% uranyl acetate for 60 s, and lastly, on three successive drops of distilled water for 5 s each. Electron micrographs of equal areas of the grids were then counted. For particle counting by the spray method, 400-mesh copper grids coated with Formvar and evaporated carbon were glow discharged shortly before spraying. The samples were dialyzed against a solution of 0.1 M ammonium acetate, 1 mM $MgCl_2$, pH 8.0. Aliquots for concomitant protein determination were always taken after dialysis. Controls containing no sample material showed that this buffer caused no detectable crystallization artifacts after spraying. Immediately before spraying, 0.25 vol of a 0.1% suspension of 91-nm polystyrene-latex spheres (Ted Pella, Inc., Tustin, CA) was mixed with the samples so that microdroplet volume could be calculated (if too much time elapsed after mixing, the latex spheres tended to aggregate). After spraying, the grids were shadowed with 100% Pt at a 45° angle. The region covered by a single drop could usually be recognized by the distribution of the sample particles and latex spheres.

In Vivo Tritium Labeling of RNA: Log-phase HeLa cells growing at densities of $5–6 \times 10^5$ cells/ml were pelleted and resuspended in 0.25 vol of fresh medium at 37°C. 15 min after resuspension, the appropriate ^{3}H-ribonucleoside (usually uridine) was added to a final concentration of 5 μCi/ml. After the appropriate labeling time (usually 20–30 min) at 37°C, the cells were pelleted and either used immediately for nuclear isolation or frozen in 50% glycerol. For 24-h labeling, [^{3}H]uridine was added to a final concentration of 0.3 μCi/ml to log-phase HeLa cells at densities $\sim 2.5 \times 10^5$ cells/ml. Cells were counted again and harvested 24 h later. This concentration of isotope was found to have little effect on the generation time of the cells (usually 24 h).

Nuclease Digestion to Generate the NRS: For routine preparation of the NRS, sonicated nuclei were incubated for 5 min at 37°C, followed by addition of 5 μg of RNase A (Sigma Chemical Co., St. Louis, MO) per 10^8 nuclei and an additional 15 min of incubation. After brief cooling on ice, chromatin and large debris were pelleted and sucrose gradient centrifugation was performed exactly as for isolation of intact 40S particles. For ribonuclease A digestion of isolated particles to generate the NRS, the 40S peak of intact particles from sucrose gradients was first dialyzed against STM buffer, pH 8.0, in order to permit immediate resedimentation on sucrose gradients after digestion. RNase A was then added in the amount of 0.12 μg/optical density (OD) 254 U of peak material from the gradients. Incubation was for 15 min at 37°. Digestion was terminated by adding RNasin (Promega Biotec, Madison, WI) to a final concentration of 1,000 U/ml and by placing on ice. For micrococcal nuclease digestion of isolated particles, intact 40S particles from

gradients were first dialyzed against 90 mM NaCl, 5 mM sodium phosphate, pH 6.8, containing 25 μM $CaCl_2$. Micrococcal nuclease (Worthington Biochemical Corp., Freehold, NJ) was then added to 3.3 U/OD 260 U of particles. Digestion was terminated by adding 0.2 M EDTA, pH 8.0, to a final concentration of 5 mM on ice.

Salt Dissociation and Reconstitution of Particles and the NRS: Either 40S intact particles or 43S NRS were taken from the peak region of a sucrose gradient and dialyzed against STM, pH 8.0, in order to permit resedimentation on gradients. Solid NaCl was added to a final concentration of either 1.0 M (for intact particles) or 0.6 M (for NRS). After 20 min aliquots of the sample to be reconstituted were dialyzed for 2 h against double STM buffer (pH 8.0) and then for an additional 2 h against STM, pH 8.0. This was followed by resedimentation on sucrose gradients as usual. To demonstrate dissociation, control gradients contained the same concentration of NaCl as the dissociated samples.

Protein Cross-linking: Sucrose gradient-purified monoparticles or nuclease-digested particles were dialyzed against cross-linking solution (10 mM sodium phosphate, pH 8.0, 0.1 M NaCl, 10 mM $MgCl_2$) overnight at 4°C. The particles were concentrated by immersion of the dialysis tube in dry Sephadex G-200 (Pharmacia Fine Chemicals, Piscataway, NJ) to the desired concentration. The cleavable cross-linking reagent 3,3′-dimethyl dithiobispropionimidate dihydrochloride (DTBP, Pierce Chemical Co., Rockford, IL) was made just before use in a 0.1 M stock cross-linking solution and titrated with 1.0 M NaOH to pH 8.0 (27, 28). DTBP was added to a final concentration range of 2.5–10 mM. The reaction was allowed to proceed at room temperature for 5–20 min and was terminated by the addition of ammonium acetate, with further incubation for 10 min at room temperature. *N*-ethyl maleimide (Eastman Chemical Products Inc., Kingsport, TN) was added to a final concentration of 50 mM from a 0.5 M stock solution in 80% ethanol. SDS was added to 0.05% to samples, that were to be directly analyzed by gel electrophoresis.

Cross-linking with the $(orthophenanthroline)_2Cu(II)$ complex (CuP) was performed at room temperature under similar conditions as described for DTBP. Equal volumes of 13.6 mM orthophenanthroline and 6.8 mM cupric sulfate in water were combined to form CuP just prior to use. CuP was added to a final concentration of 30 μM. The reaction was terminated after 3–20 min by the addition of 20 mM EDTA (pH 7.5) to 1.0 mM, followed by the addition of *N*-ethyl maleimide and SDS as described for DTBP cross-linking. In all cross-linking experiments the reagent concentration and reaction time were adjusted so that only a small percentage of the particle-associated proteins would be cross-linked. When high levels of reagent are used, the cross-linked proteins are difficult to reduce and solubilize for gel analysis. Also, in these experiments, it is important that the majority of the proteins not be cross-linked so that in the second-dimension gel, a diagonal representing the molecular weight distribution of noncross-linked protein (in the first-dimension gel) will be formed.

To identify the cross-linked species that formed under the conditions used, the particles were solubilized in sample buffer not containing mercaptoethanol and resolved in 5 mm × 10 cm cylindrical gels (26). These gels were then soaked in sample buffer containing 2-mercaptoethanol to cleave the cross-linking reagent and placed horizontally across the second-dimension slab gel before electrophoresis.

RESULTS

Nuclease Digestion of 40S hnRNP Particles and Formation of the 43S NRS

Sonically disrupted HeLa nuclei were divided into three equal aliquots and subjected to different levels of endogenous and exogenous nuclease activity prior to sucrose gradient sedimentation. To minimize endogenous nuclease activity, one aliquot was held in 0°C for 15 min prior to centrifugation (Fig. 1*A*). The second aliquot was incubated at 37°C for 15 min to facilitate endogenous ribonuclease activity (Fig. 1*B*), and the third was digested for 15 min at 37°C with ribonuclease A at 5 $\mu g/10^8$ nuclei (Fig. 1*C*). The gradients were scanned at 254 nm (upper panel) and successive fractions were analyzed for protein composition by SDS PAGE (lower panel). When isolated under conditions of minimal nuclease activity, hnRNP particles sediment in a rather heterodisperse manner with most of the material centered around a peak at 42S (Fig. 1*A*). These monoparticles contain the characteristic six major proteins (A1,A2,B1,B2,C1, and C2) described previously (2, 3, 5, 9), plus numerous higher molecular weight proteins. Mild endogenous nuclease activity (Fig. 1*B*) leads to the loss of the higher molecular weight proteins and to a less heterodisperse distribution of particles in gradients with the peak centered at 40S. The relative stoichiometry of the six major particle proteins is the same for the two cases of limited nuclease action (Fig. 1, *A* and *B*). This is also true within successive gradient fractions across the respective peaks. Digestion of the nuclear sonicate with ribonuclease A (Fig. 1*C*) leads to the loss of most of the RNA and protein. However, NRS, formed primarily of proteins A2 and B1, are observed to sediment slightly faster in gradients (43S) than intact particles and in a much more narrow zone, indicating greater structural homogeneity (also see electron micrographs below). After ribonuclease A digestion (Fig. 1*C*), >80% of

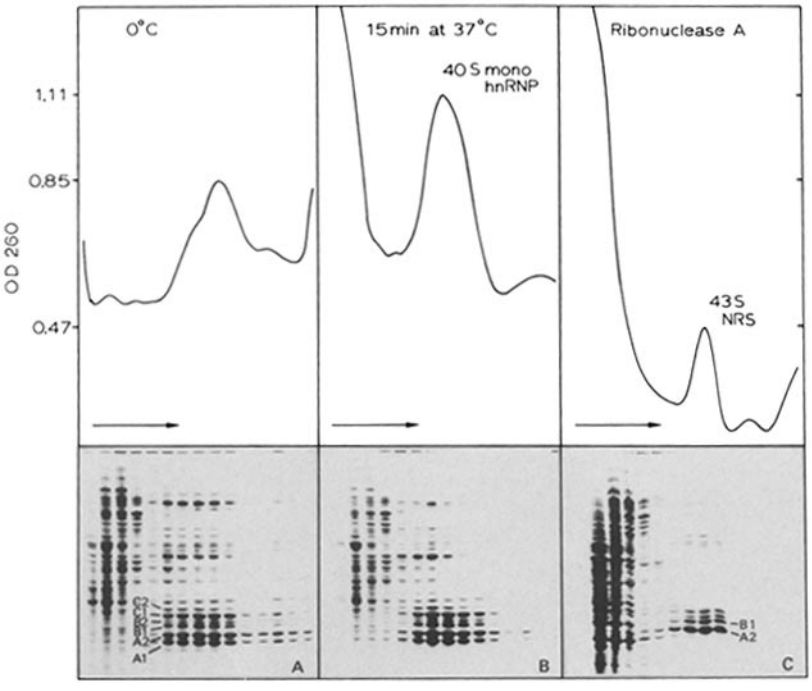

FIGURE 1 Analysis of the distribution of 40S hnRNP particle protein (*bottom*) and RNA (*top*) in 15–30% sucrose density gradients after endogenous and exogenous nuclease activity. In *A* (minimal nuclease) the protein bands denoted by the letters A1, A2, B1, B2, C1, and C2 are the major proteins of HeLa hnRNP particles with approximate molecular weights of 32,000, 34,000, 36,000, 37,000, 42,000, and 44,000, respectively (5). The peak OD 260 material shown in the upper panel is centered at 42S. *B* shows the distribution of particle proteins after endogenous nuclease is allowed to act by incubation of the nuclear sonicate at 37°C for 15 min before gradient analysis. In this gradient the peak OD 260 material is centered at 40S. C shows the distribution of protein and RNA in the NRS that form when intact hnRNP particles (*A* and *B*) are incubated in ribonuclease A as described in Materials and Methods.

the protein A2 and B1 present after endogenous nuclease action (Fig. 1 *B*) is recovered in the 43S NRS. Protein B2 and trace amounts of C1 also sediment at 43S after digestion. Proteins A1, C1, and C2, present in undigested or mildly digested particles, are dissociated by exogenous nuclease activity and remain at the top of the gradients. Endogenous nuclease will achieve the same results as ribonuclease A after lengthy incubation (15–20 h) at 37°C. Gel densitometry (not shown) reveals that the ratio of A2/B1 (3:1) is the same in the 43S NRS and in the intact monoparticles. The amount of RNA recovered at 40S increases after endogenous ribonuclease activity. This suggests that endogenous nuclease activity facilitates the additional release of 40S particles that were previously in larger structures (as components of hnRNP polyparticles or of template-associated nascent hnRNA).

The digestion conditions that generate the 43S NRS (shown in *C* of Fig. 1) typically cause the loss of at least 80% of the OD 260 material originally present in undigested 40S particles. The 43S NRS contains more total A2 and B1 protein per particle than intact 40S monoparticles due to the reassociation of $(A2)_3(B1)$ tetramers derived from three to four monoparticles (shown below). The RNA degraded during digestion contains essentially all of the sequences that can be labeled with ^{3}H-ribonucleosides (uridine, cytidine, adenine, or guanosine) during a 1-h period of exponential growth. Based on the ratio of distintegrations per minute to OD 260, the nuclease labile RNA has a 20-fold higher specific radioactivity than the RNA recovered from the NRS (data not shown). When cells are labeled for 24 h with [^{3}H]uridine, the RNA recovered from the 43S NRS has a specific radioactivity similar to total RNA isolated from intact 40S particles. We do not know whether the slowly labeled RNA recovered in the NRS is present in 40S particles prior to nuclease digestion. The slowly labeled RNA fragments remaining in the 43S NRS are ~200–220 bases in length (Fig. 2). As seen in Fig. 2, the 43S NRS generated by the action of ribonuclease A is relatively resistant to further nuclease activity; however, when digestion is allowed to proceed for 45 min at 37°C, no material is present at 43S in gradients. Instead, as described later, proteins A2 and B1 are recovered as pellets after density-gradient centrifugation. These findings demonstrate that RNA is required for the assembly and the structural integrity of the 43S NRS. The 43S NRS is also formed if 40S monoparticles are purified by sucrose gradient sedimentation, then digested with ribonuclease A. No difference in the protein composition, RNA composition, or sedimentation coefficient can be detected between the NRS formed during digestion of nuclear sonicates or of gradient-purified 40S monoparticles.

As shown in Fig. 3, essentially the same results observed using ribonuclease A are obtained with micrococcal nuclease. As digestion proceeds there is a rapid loss of the higher molecular weight proteins followed by a successive dissociation of proteins A1, C1, and C2. Trace amounts of C1 and C2 remain after 20 min of digestion. More B2 is present than in ribonuclease A-generated 43S NRS. The amount of C protein remaining with proteins A2 and B1 is a function of digestion time. As in the case of ribonuclease A digestion, 90% of the OD 260 material present in intact control particles is lost during digestion, and the NRS generated by micrococcal nuclease sediments at 43S. The data as a whole show that the 43S NRS can be generated with enzymes that cleave both single- and double-stranded nucleic acids and that NRS formation is not dependent on preferred site cleavage in the RNA. Also, the NRS may form from $(A2)_3(B1)$ tetramers or from $(A2)_3(B1)(B2)$ pentamers.

Evidence for the Peripheral Position of A1, C1, and C2

The rapid loss of RNA upon exposure of intact 40S hnRNP particles to nuclease and the coincidental loss of proteins A1, C1, and C2 suggest that these components occupy a peripheral position in 40S particles. More direct evidence for this protein arrangement has been obtained from protease digestion stud-

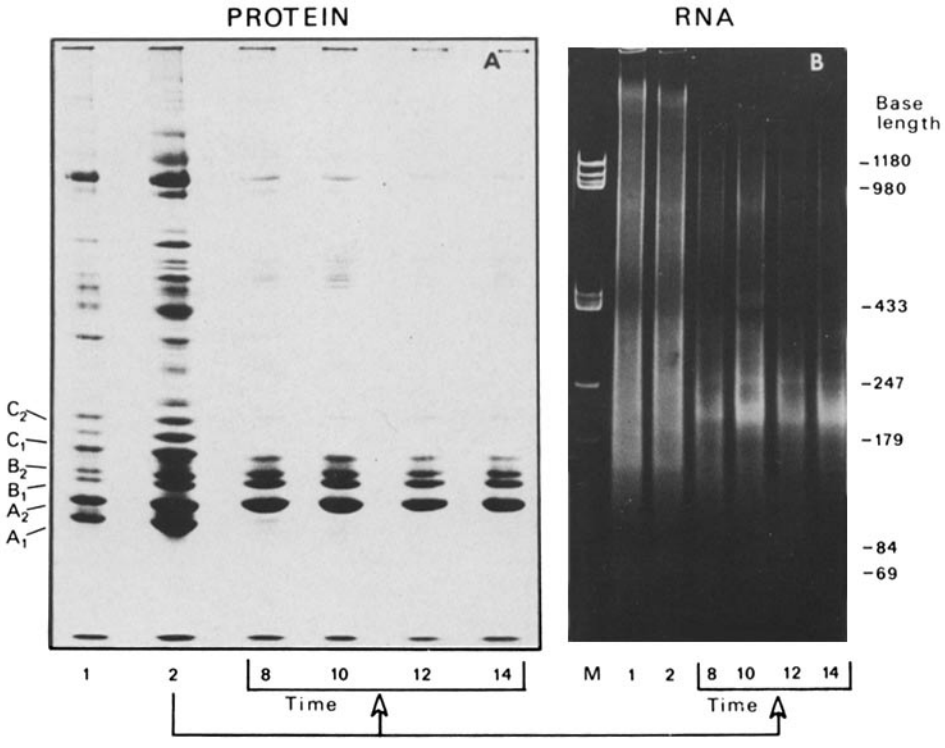

FIGURE 2 Size analysis of the RNA recovered from the 43S NRS after ribonuclease A digestion of intact 40S hnRNP particles. 40S hnRNP particles isolated from a sucrose-density gradient were digested with ribonuclease A for increasing periods of time and again resolved on sucrose gradients. The 43S peak gradient fractions containing the NRS were analyzed for protein (*left*) and RNA content (*right*). RNA was visualized with ethidium bromide (see Materials and Methods). Lane *1* of both panels corresponds to no digestion; lane *2*, digestion with endogenous nuclease for 12 min; lanes *3–6*, digestion with ribonuclease A for 8, 10, 12, and 14 min; lane *M* contains Col E1 plasmid DNA digested with Hae III (fragment size indicated at right). Note that the RNA recovered from the NRS is almost 200 bases long and that the NRS is rather stable to nuclease action over the digestion times used.

ies. Sucrose gradient-purified monoparticles were digested with trypsin, and the resistant proteins were analyzed by SDS PAGE (Fig. 4). The amount of each major protein remaining undigested after each time point was quantitated densitometrically and plotted (right panel). After 1 min of proteolysis, 90% of protein C1 was cleaved. More extensive digestion completely degraded the C proteins and A1, followed by A2 and B1, which are more resistant to trypsin. Digestion of isolated 40S particles with chymotrypsin reveals the same order of sensitivity despite the difference in cleavage site specificity of the two enzymes (described in reference 29). This observation indicates that the differential protein sensitivity observed is most likely due primarily to protein arrangement in particles rather than to differences in amino acid composition (for example, see reference 30).

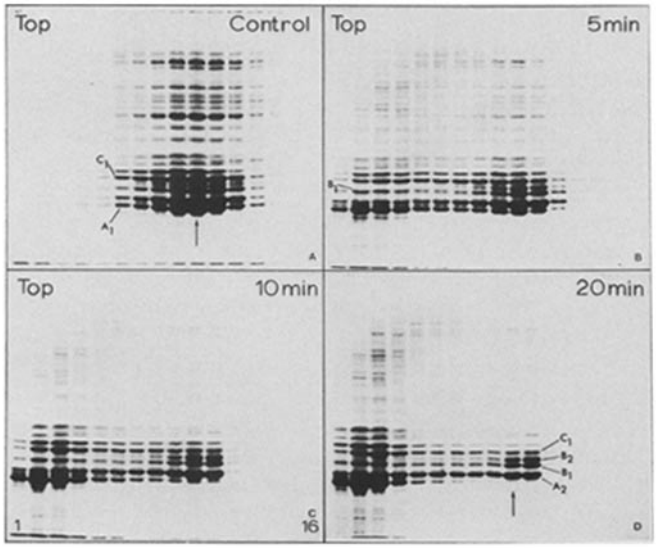

FIGURE 3 The effects of micrococcal nuclease on hnRNP particle composition and formation of the 43S NRS. Gradient-purified 40S particles were digested with 3.3 U of micrococcal nuclease per OD 260 unit for 5, 10, and 20 min at 37°C. The reaction was terminated with buffered EDTA (see Materials and Methods) and the resulting material was sedimented through 15–30% sucrose gradients. The arrows denote the 40S position of the gradients as determined by co-sedimentation of particles with 30S and 50S *Escherichia coli* ribosomal subunits. Note that as in the case of ribonuclease-generated NRS, those generated by micrococcal nuclease also sediment at 43S. In this figure the top of each gradient is to the left.

Further evidence that the differential digestion rate observed is not due to primary sequence differences among the various proteins was obtained in control experiments in which monoparticles were dissociated in 0.8 M NaCl (shown previously to solubilize the particle proteins [4]) and then exposed to trypsin or chymotrypsin. In these experiments no measurable difference in specific protein digestion rate could be detected. In contrast, as seen in Fig. 4, in intact particles proteins A2 and B1 are resistant to protease activity. Additional evidence for their shielded position in intact particles can be seen in experiments in which isolated 43S NRS were digested in parallel with intact monoparticles. The extent of A2 and B1 cleavage in both structures was quantitated with time (Table I). In these experiments total protein was equalized in both samples and trypsin was added at 0.01 μg/mg of protein to circumvent the digestion rate difference as a function of substrate concentration. After 1 min of digestion, proteins A2 and B1 in isolated 43S NRS are 20-fold more sensitive to trypsin than are the same proteins in intact particles. After 2 min of digestion nearly 33% of the A2 and B1 in intact particles persists, while only trace amounts of these proteins remain uncleaved in the isolated NRS (Table I).

To determine whether the sterically protected proteins A2 and B1, which remain after limited protease digestion, exist as a particulate structure, a preparation of isolated 40S monoparticles was purified by sucrose density-gradient centrifugation, and then divided into six equal aliquots. Five aliquots were digested with trypsin for 1, 3, 6, 9, or 12 min, and then resedimented. The undigested control is shown in the upper left panel of Fig. 5. Note that after 3 min of digestion most of the high molecular weight protein as well as the C proteins have been cleaved. In this sample the peak gradient fractions are essentially the same in protein composition as the early

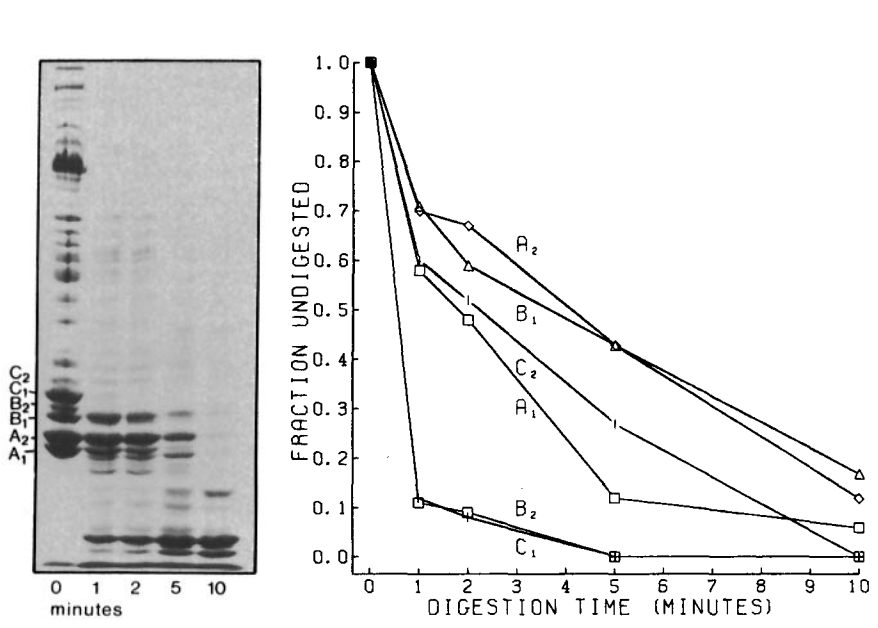

FIGURE 4 Preferential proteolysis of 40S hnRNP particle proteins. Sucrose gradient-purified 40S hnRNP particles (lane *0*) were digested with 0.005 μg trypsin/μg of particle protein for 1, 2, 5, and 10 min at 37°C. Soybean trypsin inhibitor was used to terminate proteolysis and the proteins were resolved electrophoretically (*left*). The cleavage of individual proteins was followed with time densitometrically and plotted (*right*). In separate experiments two-dimensional gel electrophoresis was used to ensure that during proteolysis cleavage products of the higher molecular weight proteins do not co-migrate with the major particle proteins in lanes *2–5* (29).

TABLE I

Comparative Trypsin Digestion of 40S Monoparticles and NRS

Digestion time	40S hnRNP	43S NRS
min	*percentage of A2, B1, and B2 undigested*	
0.0	100	100.0
0.5	63	60.0
1.0	43	2.0
2.0	19	0.5
5.0	3	0.0

digestions seen in Fig. 4. After 6 min of digestion, A2 and B1 are the major proteins remaining and, as in the case of nuclease digestion, these proteins are present at nearly a 3:1 molar ratio. Unlike the NRS, the trypsin-resistant structures sediment slightly slower than intact particles and retain more protein A1 than is observed in nuclease generated NRS. After 9 min only trace amounts of A2 and B1 can be seen (Fig. 4). After 12 min no protein can be detected in gradient fractions (gel not shown). To demonstrate that these results are not due to nuclease in the trypsin used, monoparticles were isolated from cells labeled for 1 h with [^{3}H]uridine and total acid precipitable counts were determined immediately on half of the preparation. No significant decrease in precipitable counts was observed after incubating the second half in the presence of trypsin for 45 min.

Protein Stoichiometry and Identification of the Major Homotypic Protein Associations in 40S hnRNP Particles

When nuclear 40S hnRNP particles are isolated from exponentially growing HeLa cells, gel densitometry reveals that proteins A1, A2, and C1 are apparently present at a 1:1:1 molar ratio (see Figs. 1 and 3–5; scans not shown). As demonstrated above, the peripheral proteins A1 and C1 preferentially dissociate as the particle-associated RNA is cleaved with nuclease; these two proteins are also the most labile to protease. For these reasons the equimolar ratio for the three major proteins only holds for particles not subjected to nuclease or protease activity. Also, as shown previously (9), protein A1 diminishes as cell growth slows and only trace amounts of A1 can be recovered from tissues containing mostly G_0 cells (31). Intact particles that possess the 1:1:1 ratio among A1, A2, and C1 reveal a 3:1 ratio between these proteins and the B group proteins. Perhaps due to varying degrees of posttranslational modification (12, 16, 32), protein B2 sometimes resolves into a closely spaced doublet and frequently is present in amounts less than B1. Proteins C1 and C2, which are very similar based on physical chemical (2, 5, 9, 33) and immunological (34) criteria, usually are present at a 3:1 ratio but C2 varies between 25–33% of the amount of C1.

Even when care is used to ensure that particles are isolated from exponentially growing cells under conditions of minimal nuclease and protease activity, and when protein loads are adjusted to yield bands in their linear dye-binding ranges, experimental variation contributes to densitometric values between 2.8:1 and 3.4:1 for the ratio of proteins A2 and B1. There may also be differences in the extent of dye binding and the extinction coefficient for bound dye among the six polypeptides. Cross-linking studies, described below, provide the most convincing evidence that proteins A1, A2, and C1 are present at equimolar amounts in particles and that proteins A2 and B1 exist as a tetrameric complex. These studies reveal that A1, A2, and C1 each exist as homotypic trimers in intact particles.

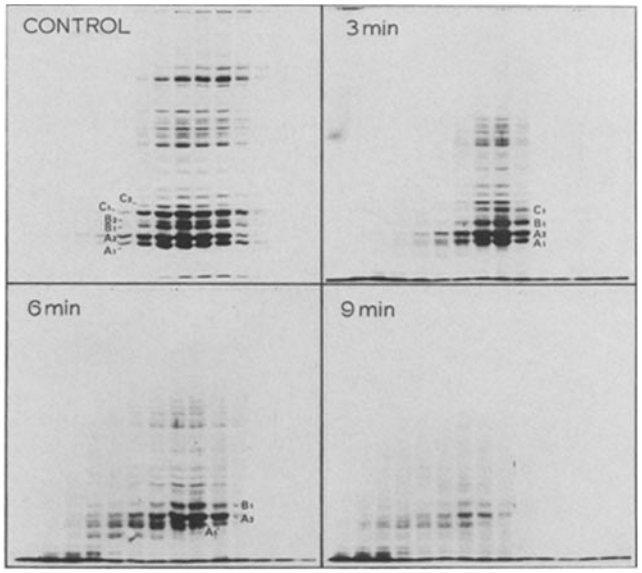

FIGURE 5 The effects of proteolysis on the sedimentation properties of hnRNP. As shown in Fig. 4, proteins A1, C1, and C2 are preferentially cleaved when intact 40S particles are exposed to protease. In this figure it can be seen that the order of protein digestion is the same but also that the sterically shielded proteins A2 and B1 continue to sediment as a particulate structure though slightly slower than intact particles. The top of each gradient is to the left in each panel.

The nearest neighbor contacts among the major particle proteins were identified through the use of cleavable cross-linking reagents that covalently bind adjacent proteins. The reagent DTBP is a homobifunctional cross-linking reagent that acts by amidinating primary amino groups (27, 28) spaced within 1.1 nm of each other. A central disulfide bridge in the reagent may be cleaved by reduction with reagents such as 2-mercaptoethanol. Thus the proteins present in a cross-linked complex can be identified by electrophoresis after reduction. The second reagent used in these studies (orthophenanthroline)$_2$Cu(II), or CuP, catalyzes the formation of disulfide bridges between existing reduced cysteine residues in the proteins. This reagent is thus a zero-length reversible cross-linker.

Identification of the proteins in cross-linked complexes was accomplished by two-dimensional gel electrophoresis following the method of Wang and Richards (27, 28), modified by incorporating an SDS-polyacrylamide gel system described previously (26). The results obtained when DTBP is used as the cross-linking reagent are shown in Fig. 6. The upper and lower panels show the second-dimension slab gels of control and cross-linked particles. In these gels the proteins that were cross-linked (and ran as higher molecular weight complexes in the first-dimension gel) run to the left of and below the diagonal formed by the proteins not cross-linked during the experiment. Molecular weight standards and samples of hnRNP are included in both gels as an internal reference. It can be seen in the lower panel that proteins A1, A2, and C1 are cross-linked by DTBP such that the major cross-linked species are trimers of each protein. As would be expected, smaller amounts of dimeric complexes and evidence for het-

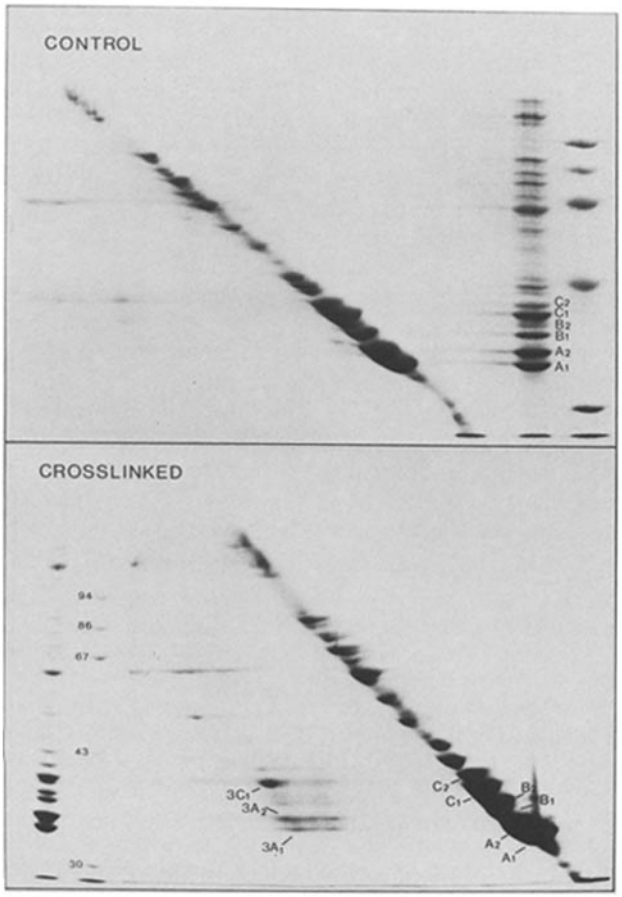

FIGURE 6 Analysis of DTBP-crosslinked monoparticle proteins by two-dimensional gel electrophoresis. Monoparticles were dialyzed in phosphate cross-linking solution and divided into two equal aliquots. One aliquot was treated with 2.5 mM DTBP for 15 min at room temperature (*bottom*); the other aliquot is the untreated control sample (*top*). Both samples were subjected to two-dimensional electrophoresis to determine the presence of cross-linked complexes. The cross-linking reagent was cleaved with 2-mercaptoethanol before the second-dimension slab gels shown here were run. Samples of intact 40S particles and molecular weight standards were applied to the slab gels for internal reference. Proteins cross-linked in the first-dimension gel run as spots below the diagonal (*bottom*). The proteins present in cross-linked complexes are identified by their molecular weights × 10^3. The number of copies of each protein present in a cross-linked complex can be calculated from their molecular weights and the molecular weight of the complex. The major cross-linked species are trimers of A1, A2, and C1 (see Results). Molecular weight markers are carbonic anhydrase (30,000), ovalbumin (43,000), bovine serum albumin (67,000), conalbumin (86,000), and phosphorylase B (94,000).

erotypic complexes (to the right of the three major spots) can be seen. Because proteins A1 and A2 differ in molecular weight by only 2,000, it is not possible to identify with certainty the heterotypic contacts that exist; however, the vertically positioned spots of A1 and A2 (to the right of the major spots) indicate that A1 and A2 are in contact in intact monoparticles. It also appears that heterotypic contacts exist between the B proteins and the A or C group proteins, but again the molecular weights of these proteins are not sufficiently different to identify the heterotypic contacts with certainty. To the left of the three major spots in the lower panel, trace amounts of protein can be seen, suggesting that trimers of these proteins are associated with other trimers within intact particles. In the upper control panel small amounts of the C proteins can be seen to have spontaneously formed trimeric complexes. This is consistent with our findings that CuP (which catalyzes the formation of disulfide crossbridges between proteins in contact) very effectively cross-links the C group proteins (data shown in reference 29).

The results shown in Fig. 6 are also obtained when the NRS is cross-linked with DTBP or CuP. As in Fig. 6 the darkest B1 spot is just above and at the left most edge of the major A2 spot. This is consistent with the possibility that some heterotypic tetrameric associations are present. In these experiments negative results cannot be interpreted as evidence for the absence of a particular protein contact, since cross-linked complexes are dependent on the steric placement of reactive sites. With the reagents used in this study, evidence for contacts between the A and C group proteins was not obtained. It seems unlikely, however, that contacts do not occur between these proteins given their equimolar ratios and the fact that they are present in the same structure. Cross-linked complexes between the major particle proteins and the higher molecular weight components are also not observed. A tetrameric association of $(A2)_3(B1)$ in the NRS is indicated by the observations that in highly purified NRS, A2 and B1 comprise at least 90% of total NRS protein; they are present in a 3:1 molar ratio; the A2 trimer is easily demonstrated with DTBP and CuP; and as shown later, the NRS dissociates into smaller structures which retain the 3:1 ratio.

Evidence That the NRS Forms Via Tetramer Rearrangement

As shown above, the nuclease- or protease-induced loss of the peripheral proteins (A1,C1, and C2) and 90% of the RNA associated with intact 40S monoparticles leads to the generation of a faster-sedimenting NRS composed primarily of proteins A2 and B1 in a 3:1 molar ratio. Depending on the extent of digestion, the protein and RNA lost during NRS generation accounts for 60–80% of the original mass of intact particles. Evidence that the NRS is formed by a highly specific rearrangement of protein is derived from quantitative electron microscopic observations, mass estimates, and other observations summarized in Discussion.

In the ultrastructural studies performed, two procedures were used to determine the number of NRS that derive from a given number of intact particles during nuclease digestion. Since the majority (typically 70–75%) of the protein A2 initially present in an intact particle preparation is recovered in the NRS peak after digestion, all particle counts were corrected for A2 loss in each experiment and for sample volume differences.

In the first procedure (adsorption), nuclear sonicates were divided into two equal aliquots. One aliquot was held on ice while the other was digested at 37°C for 15 min with ribonuclease A (5 $\mu g/10^8$ nuclei) to generate the 43S NRS (see Materials and Methods). After sucrose-gradient sedimentation the monoparticle and 43S NRS peak fractions were pooled separately, their respective volumes were measured, and aliquots were taken for protein A2 quantitation. The remaining material was used for electron microscopy. Formvar and evaporated carbon-coated grids were allowed to float on 50-μl drops of sample for 1 min and excess liquid and washes were drawn off by capillary action (see Materials and Methods). The grids were stained with uranyl acetate and photographed at ×30,000.

In typical experiments three photographs were taken at random from each of two grids for intact particles and NRS samples. An 18 × 24-cm ruled transparency was placed over prints representing a total magnification of ×120,000 and each particle or NRS was marked and independently counted twice. The results from one of the experiments are shown in Table II. In this experiment direct counts revealed 1.85 times as many intact particles as NRS (235 monoparticles to 127 NRS). After correcting for protein A2 recovery and sample volume differences, we calculate that there were 3.3 times more intact particles than NRS. This value was also obtained as the average of three similar experiments. Stated in another way, the $(A2)_3(B1)$ tetramers present in one NRS are derived from approximately 3.3 monoparticles. Due to some experimental variation (i.e., a ratio of 4.4:1 was obtained as the highest value), we cannot determine whether the tetramers that reassociate to form the NRS are derived from three or four monoparticles after appropriate corrections are made. If this number were known, it would be possible to determine with greater precision the copy number of the major components in 40S hnRNP particles.

TABLE II

Counts of Intact Particles and NRS

Sample	Grid	Count average	SD	Average for preparation
Particles	D1	249	12.0	
	D1	227	2.5	
	D1	223	10.0	
	D2	234	1.0	
	D2	227	14.0	
	D2	249	2.0	235 particles ± 11.5
NRS	E1	130	3.0	
	E1	128	2.5	
	E1	128	5.0	
	E2	122	1.5	
	E2	126	1.5	127 NRS ± 3.4

The results described above are valid if major differences do not exist in the respective affinity between intact particles and NRS for the electron microscopic grids rendered hydrophilic by glow discharge. Ratios in the same range as above were obtained when hydrophobic grids (i.e., not glow discharged) were used, and no significant difference was observed when adsorption times were varied. In an effort to circumvent the potential artifact that could arise from differential grid adhesion, grids were prepared by the spray droplet method of Dubochet and Kellenberger (35) that used polystyrene beads to monitor droplet volume. In these experiments particles were equilibrated by dialysis in volatile ammonium acetate buffer prior to spraying the grids. After numerous procedural modifications, we were not able to prevent particle aggregation, particle dissociation, and in other cases, artifacts due to surface denaturation. The spray droplet method generally yielded ratios in the range of 5–6:1 (intact monoparticles to NRS). Although we believe these data are less accurate than those obtained through the adsorption procedure, the results are mentioned to point out that, as in the adsorption method,

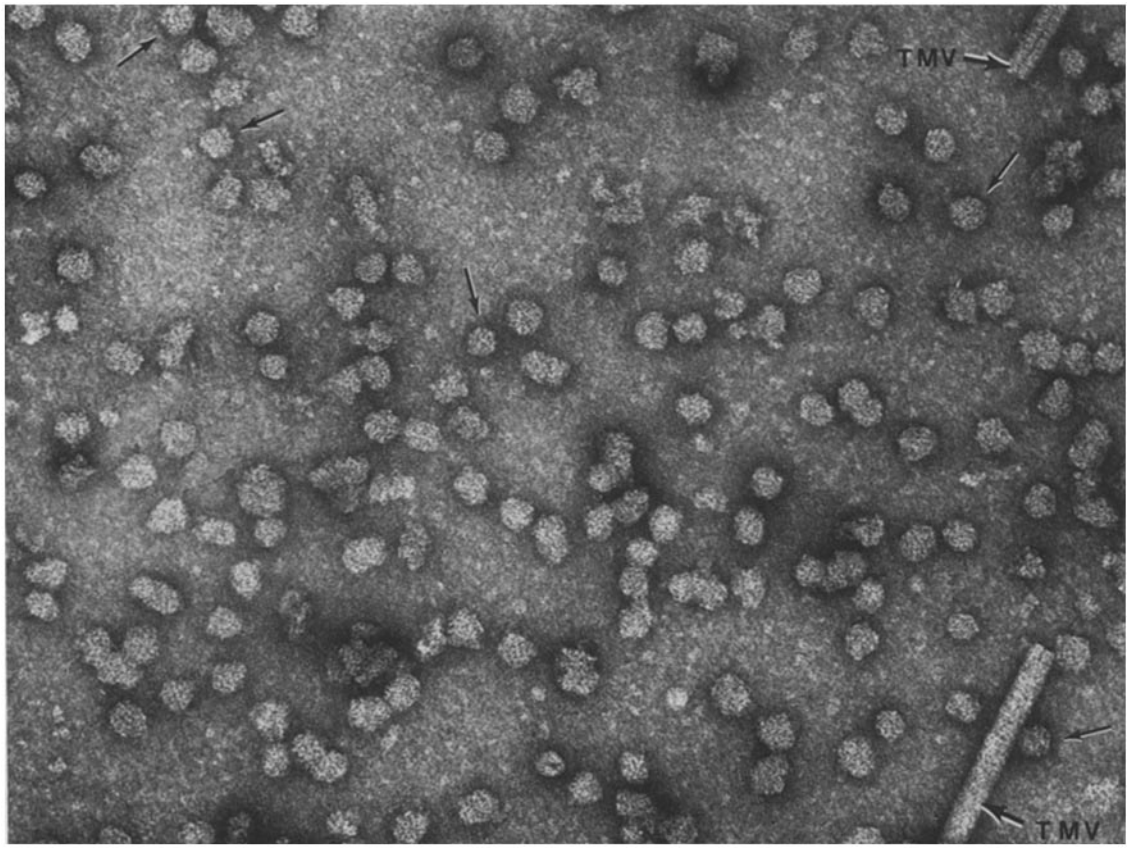

FIGURE 7 Electron micrograph of the 43S NRS. Peak 43S sucrose-gradient fractions were pooled, dialyzed against STM to remove sucrose, fixed in 0.1% glutaraldehyde 5 h, and negatively stained with 1% ammonium molybdate. Tobacco mosaic virus (*TMV*) is included as an internal size standard. In this electron micrograph the viral filaments have a diameter of 20 nm based on 2.6 nm per stacked disk. The 43S NRS vary from 20 to 22 nm. The arrows denote those particles that appear icosahedral (six sided) in shape.

fewer NRS than intact particles are always observed after nuclease digestion.

Observations that support the hypothesis that the particulate NRS are composed of a fixed number of tetramers are their size homogeneity observed in electron micrographs (Fig. 7), their narrow band of sedimentation in gradients (Fig. 1), their symmetrical and narrow zone of elution from gel filtration columns (described below), and in negatively stained preparations, the appearance of a significant number of particles that show six-sided symmetry (Fig. 7). Further evidence that tetramers can reassociate to form highly ordered structures is seen in their ability to form extremely long spiral filaments with a diameter of 18–20 nm and a pitch near 60 nm (Fig. 8). These filaments form when isolated NRS are equilibrated in 0.1 strength STM buffer. The filaments can be recovered as pellets from the bottom of 15–30% sucrose gradients. As digestion proceeds, the ratio of filaments to NRS increases. In addition, after extensive nuclease digestion of isolated NRS, pellets contain few if any NRS particles, yet proteins A2 and B1 comprise essentially all of the protein recovered from this filamentous material. As in the case of the globular NRS, proteins A2 and B1 are also present at a 3:1 molar ratio in the filaments. Once formed the filaments cannot be dissociated by 2.0 M salt. A detailed characterization of these structures will be described in a separate paper.

Physical Properties of the NRS

As expected from the disproportionate loss of protein and RNA during generation of the NRS, the buoyant density of the NRS is less than that of monoparticles. Fig. 9 shows the position of glutaraldehyde-fixed 40S monoparticles (*A*) and the NRS (*B*) in cesium chloride gradients. Intact monoparticles have a density of 1.384 g/cm^3, compared with 1.361 g/cm^3 for the NRS. In both determinations, protein and RNA co-sediment, indicating efficient fixation and no significant amount of salt-induced dissociation. Using 1.9 g/cm^3 for the density of RNA and 1.32 g/cm^3 for the density of aldehyde-treated protein (36) and the formula of Spirin (37) for calculating protein to RNA ratios, intact particles possess a protein to RNA ratio of 8:1 and of 13:1 for NRS. We have also determined the protein and RNA content of intact particles and the NRS biochemically. Protein determinations via the Lowry assay (38) and OD 260 measurements for RNA quantitation yield ratios of 8.3:1 for intact particles and 14.5:1 for the NRS, values in close agreement with the calculation above based on the gradient data.

Gel filtration chromatography of both intact 40S hnRNP particles and the NRS (Fig. 10) show little difference between the Stokes radius of these two structures. The NRS elutes with an estimated mass of 2.2–2.3 million. In Fig. 10 the protein composition of the peak eluting material is shown. The peaks of OD 260 material at the exclusion volume contain little or no protein and are composed of free RNA. Preliminary mass analyses by scanning transmission electron microscopy place the NRS mass somewhat lower at roughly 2.0×10^6.

As observed previously for intact 40S hnRNP particles (5, 12), 0.6 M salt-dissociated NRS can be reconstituted via dialysis back to 0.1 M salt (Fig. 11). A significant observation in these studies is that during handling there is a spontaneous

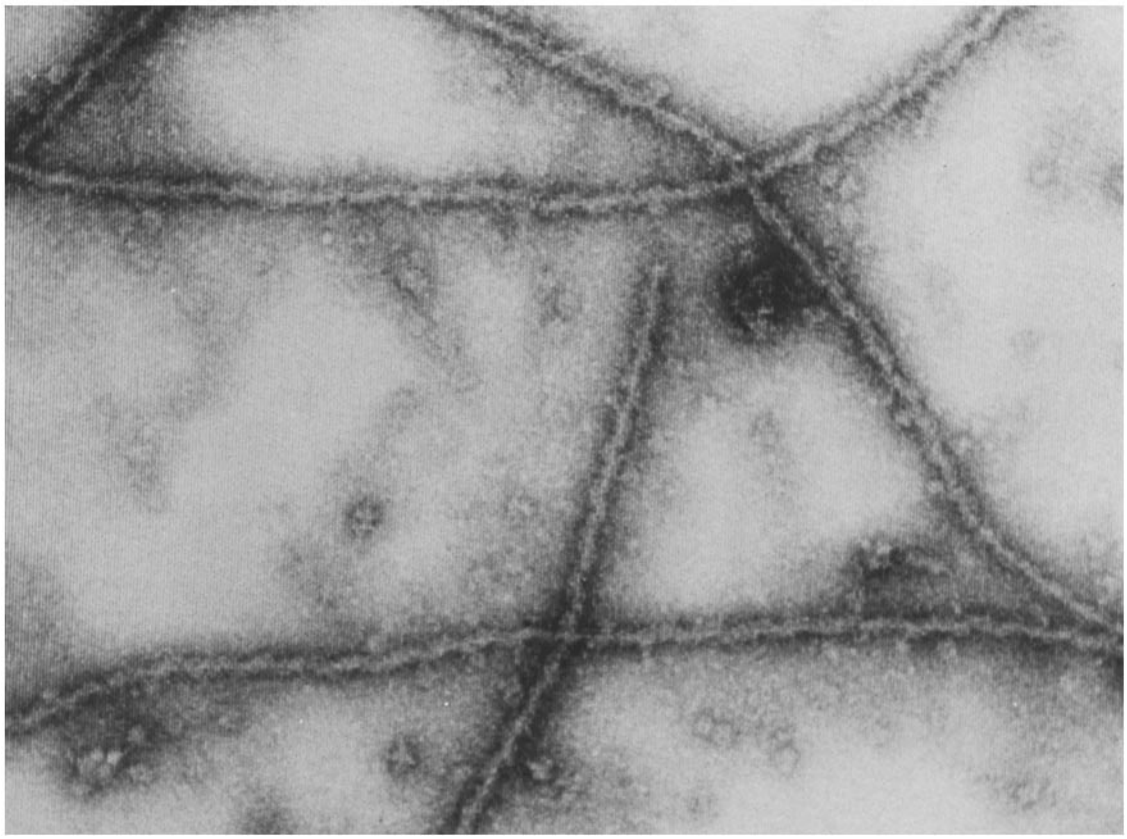

FIGURE 8 Filaments formed from NRS by equilibration in low ionic strength solution. These helical filaments are of indefinite length with a diameter 18–20 nm and a pitch near 60 nm. The filaments are not dissociated in 2.0 M NaCl and are composed almost entirely of proteins A2 and B1 in a 3:1 molar ratio. The filaments were fixed with 0.1% glutaraldehyde, negatively stained with uranyl acetate, and photographed with the scanning transmission electron microscope. × 110,000.

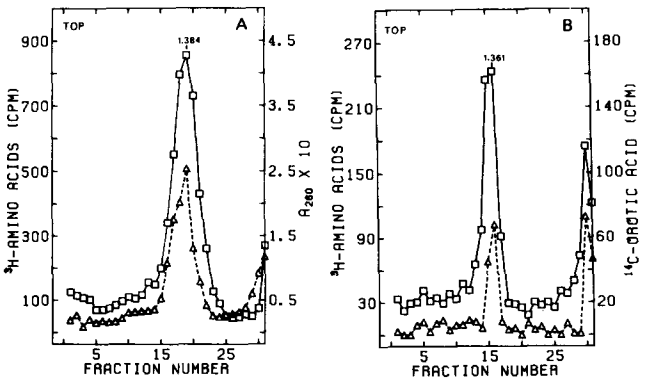

FIGURE 9 Isopycnic centrifugation of monoparticles (*A*) and the NRS (*B*) in cesium chloride. Sucrose gradient-purified 40S particles (labeled with ^{3}H-amino acids) were fixed in 0.2% gluteraldehyde for 6 h on ice. The sample was dialyzed against STM, pH 8.0, to remove unreacted glutaraldehyde, and then concentrated 10-fold. The particles were laid atop 10.5 ml of 38% cesium chloride in STM pH 8.0 and subjected to centrifugation at 40,000 rpm for 65 h at 4°C in a type 65 rotor (Beckman Instruments, Inc.). The gradient was fractioned into 0.4-ml aliquots. The position of protein was determined by scintillation counting (squares) and RNA by absorbance at 260 nm (triangles). Density was determined by conversion from the refractive index of each sample. The NRS (*B*) were labeled with [^{14}C]orotic acid (triangles) and ^{3}H-amino acids (squares) and were fixed and subjected to isopycnic centrifugation using the conditions described above.

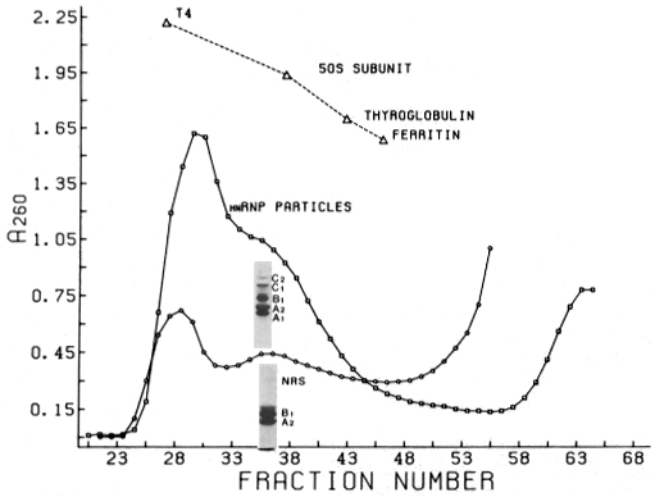

FIGURE 10 Bio-gel A-5$_M$ gel filtration chromatography of monoparticles and the NRS. A nuclear sonicate containing intact 40S monoparticles was concentrated to a volume of 1.4 ml and eluted through a Bio-gel-A5M column (—□—). 0.95-ml fractions were collected and analyzed for protein content by gel electrophoresis. Absorbance at 260 nm was measured for all fractions. The column was calibrated by co-elution of particles with T_4 phage, the 50S ribosomal subunit, thyroglobulin, and ferritin. The 40S particles eluted symmetrically about a peak centered at fractions 35–37. The proteins present in the peak fraction are shown in the upper insert. The same experimental conditions were used for gel filtration of the NRS (- - -○- - -). Only trace amounts of protein were present in the void volume OD 260 peak at fraction 28. The proteins present in the NRS peak at fractions 35–37 are shown in the lower insert.

dissociation of isolated NRS into smaller structures which can be seen to smear to the top of gradients to *A* and *C* of Fig. 11. The lighter-sedimenting fragments retain the 3A2 to 1B1 ratio pointing to the stability of this fundamental protein association. The movement of protein into the upper most

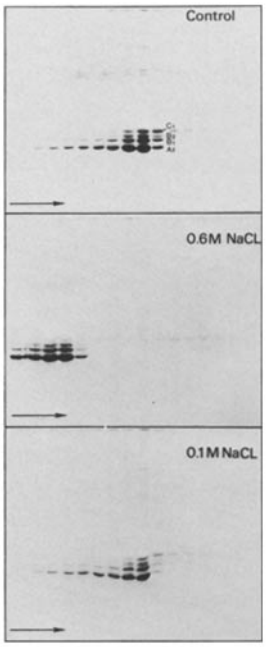

FIGURE 11 Dissociation and reconstitution of the NRS and evidence for the presence of subunits retaining the 3:1 stoichiometry of proteins A2 and B1. NRS were prepared by following procedures outlined in Materials and Methods except that in this case somewhat less RNA cleavage was achieved (i.e., higher levels of B2 and C1 present). The preparation was divided into three equal aliquots. Two aliquots were brought to 0.6 M STM (pH 8.0) to effect dissociation and the control sample (*top*) was held on ice in 0.1 M STM. One of the 0.6 M STM samples was dialyzed for 8 h against 0.1 M STM to allow for NRS reconstitution. The control and reconstituted samples were sedimented through sucrose-density gradients containing 0.1 M STM. The dissociated sample (*middle*) was sedimented through a gradient containing 0.6 M STM throughout. Note in the control and reconstituted samples (*top* and *bottom*) that the NRS dissociates into smaller structures, which can be seen to trail to the 5–10S region of the gradients, and that at 0.6 M STM complexes presumably of $(A2)_3(B1)$ enter the gradients and sediment at ~10S.

gradient fractions (Fig. 11 *B*) suggests that tetramers persist in 0.6 M salt. Bovine serum albumin, for example, only enters the first two gradient fractions under the same experimental conditions. The salt-resistant nature of the tetramer is consistent with the fact that the helical filaments formed of these proteins cannot be solubilized at 2.0 M NaCl.

DISCUSSION

As shown above, 40S ribonucleoprotein particles prepared under conditions of minimal nuclease and protease activity from exponentially growing HeLa cells possess a 1:1:1 molar ratio of proteins A1, A2, and C1, and a 3:1 ratio between these proteins and the B group proteins and C2. Protein cross-linking studies show that proteins A1, A2, and C1 exist as homotypic trimers in intact particles. This observation supports the general stoichiometry stated above and also the 3:1 relationship between proteins A2 and B1, which constitute 75–80% of the protein mass of the 43S NRS and >90% of the protein present in the helical filaments formed by these proteins. Although homotypic trimeric protein associations are not common, the tail spike proteins of *Salmonella* phage 22 show interesting phenomena in common with the trimers of 40S particles. The tail spike proteins of P-22 assemble to form very stable trimers, which are not easily dissociated with salt or SDS, are rather resistant to trypsin, and migrate in SDS gels with a molecular weight less than three times the molecular weight of the individual polypeptides (39). The trimers of protein A2, which interact with B1 to form the 43S NRS and the helical filaments described here, are resistant to high salt dissociation. If samples are not boiled in SDS-mercaptoethanol prior to electrophoresis, aggregates of these proteins appear in the high molecular weight regions of gels. Also like the P-22 trimers, the trimers of A1, A2, and C1 prepared from monoparticles migrate with molecular weights less than expected from their monomeric molecular weights.

Observations supporting the formation of the 43S NRS by a highly specific reassociation of $(A2)_3(B1)$ tetramers are: (*a*) the agarose elution profile and thus apparent mass (2.25 million) of the NRS is similar to that of intact particles despite a 70–75% loss of mass from 40S particles during nuclease digestion; (*b*) intact 40S particles yield three to four times fewer NRS after nuclease digestion despite a 70–80% recovery of total protein A2 and B1 in the latter; (*c*) the NRS sediments faster in gradients than intact 40S particles and calculations show that this cannot easily be explained by a decrease in frictional coefficient alone (if the NRS preexisted within 40S particles); (*d*) two different structures cannot be resolved from crude hnRNP preparations in sucrose or cesium chloride gradients; (*e*) when 40S hnRNP preparations are run on sucrose-density gradients, an enrichment of the NRS proteins A2 and B1 is never observed at 43S in spite of the tight zone of sedimentation observed for the 43S NRS, that is, the molar ratios of the six major proteins are conserved across the entire gradient; and (*f*) isolated NRS spontaneously dissociate with time into smaller slower sedimenting fragments, each retaining the $(A2)_3(B1)$ stoichiometry. This last observation clearly indicates that the NRS is composed of some multiple of these tetramers.

The above findings demonstrate that two types of particles (nuclease resistant and nuclease labile) do not exist in 40S particle preparations and that the NRS is an artifactual rearrangement product rather than an internal structure common to each monoparticle. However, based on the nuclease and protease studies described in Results, the major protein components of the NRS (A2 and B1) are positioned internally in intact particles. Although the NRS does not exist prior to nuclease digestion, its characterization has provided useful information regarding monoparticle composition and structure. For example, the copy number of the major proteins and the number of tetramers in the NRS and in intact monoparticles can be approximated. In these calculations the protein mass of the NRS (2.1 million) is obtained by subtracting the RNA mass (1.61×10^5) from 2.25 million (the mass of the NRS via gel filtration). The mass of the RNA subtracted is based on a 14:1 protein to RNA ratio calculated from the buoyant density of the NRS and through chemical assay. If the molecular weights of the protein components of the NRS (A2, B1, B2, traces of C1, and two very minor high molecular weight proteins) are multiplied by their respective molar ratios (via densitometry) and combined, the molecular weight of a $(A2)_3(B1)$ tetramer plus the associated B2 protein is 1.73×10^5. The multiple of this value, which essentially equals the protein mass of the NRS, is 12 (yielding 2.1 million). If 12 tetramers do in fact constitute an NRS, this would be supportive of icosahedral shape and dodecahedral symmetry. A significant number of regular six-sided structures are routinely seen in electron micrographs (Fig. 7). Neither 11 nor 13 tetramers seem consistent with a regular, ordered reassembly product.

If the copy number of proteins A2 and B1 in the NRS is 36 and 12, respectively (i.e., from 12 tetramers), and if these proteins are derived from three or four intact 40S particles during nuclease digestion, then intact particles would contain four or three tetramers, respectively. The mass of intact particles can be calculated for each case as follows. If four tetramers are present in intact monoparticles then, from intact particle protein stoichiometries, there must be 12 copies of A1, A2, and C1 and four copies of B1, B2, and C2, yielding a protein mass for these components alone of 1.76 million. If the mass of the minor higher molecular weight proteins (21% of 40S hnRNP protein mass) is added as well as the RNA mass of intact particles (calculated from the 8:1 ratio), then monoparticle mass would be near 2.5 million. Monoparticles composed of three tetramers would possess a mass of 1.9 million. Depending on their shape and density, particles with either of these masses could possess a sedimentation coefficient near 40S.

In summary, the findings reported here suggest that, when isolated under conditions of minimal nuclease and protease activity, intact 40S monoparticles are composed of repeating structural units themselves composed of 3A1, 3A2, 1B1, 1B2, 3C1, and 1C2. During 40S particle formation three or four of these structural units assemble in such a way that stable tetramers of $(A2)_3(B1)$ are positioned internally to the C proteins and to protein A1. As demonstrated here, most of the RNA is positioned in a peripheral nuclease-labile manner. This RNA must be present for the peripheral proteins A1, C1, and C2 to exist in association with the tetramers of $(A2)_3(B1)$. When the peripheral RNA is removed by nuclease digestion, approximately 12 tetramers of $(A2)_3(B1)$ reassociate in 0.1 M salt to form highly regular 43S NRS with a mass near 2.1 million and with icosahedral shape. The ocurrence of two 200–220-base, slowly labeled RNA fragments in each 43S NRS is not presently understood. The slowly labeled fragments may be derived from a slowly labeled, 2.4-kilobase RNA species that co-migrates in gradients with 40S monoparticles. This possibility and the nature of the RNA is currently under investigation. When isolated 43S NRS are equilibrated in low ionic strength solutions, an indefinite number of tetramers associate to form highly symmetrical, long spiral filaments. In some cases (25) these filaments may have been interpreted as elements of a nuclear matrix. More importantly, a study of the 43S NRS and the spiral filaments described here may yield additional information on the protein copy number and organization of protein and RNA in intact 40S hnRNP particles.

Emphasis in this report has been placed on the $(A2)_3(B1)$ tetramers as a stable protein arrangement in monoparticles, the NRS, and the insoluble helical filaments. Because the NRS could form from pentamers of $(A2)_3(B1)(B2)$ (see Figs. 2 and 3) and because varying amounts of B2 are usually present in typical NRS preparations, a pentamer of these proteins may actually exist in intact 40S particles.

The experimental results described here, which show that most of the particle-associated RNA and proteins A1, C1, and C2 occupy a peripheral position in intact particles, are supported by the recent findings of Dreyfuss and colleagues (34), demonstrating that monoclonal antibodies to the C proteins specifically immunoprecipitate relatively intact hnRNP complexes and monoparticles. Furthermore, these investigators have shown that the peripheral proteins (whose presence is dependent on RNA) readily cross-link to particle-associated RNA in vivo by a brief ultraviolet irradiation of viable cells (40).

We thank Douglas Smythe, Amy Kells, and Milton Brice for excellent technical assistance. We thank Dr. Robert Bird for his helpful discussions and for supplying Col E1 plasmid. We thank Dr. Joseph Wall for advice and discussions concerning the scanning transmission electron microscopy.

This work was supported by National Science Foundation grant PCM-8209420 to Dr. LeStourgeon.

Received for publication 24 October 1984, and in revised form 8 January 1985.

REFERENCES

1. Pederson, T. 1974. Proteins associated with heterogeneous nuclear RNA in eukaryotic cells. *J. Mol. Biol.* 83:163–183.
2. LeStourgeon, W. M., L. Lothstein, B. W. Walker, and A. L. Beyer. 1981. The composition and general topology of RNA and protein in monomer 40S ribonucleoprotein particles. *In* The Cell Nucleus: Nuclear Particles, Vol. 9, Part B. H. Busch, editor. Academic Press, Inc., New York. 47–87.
3. Walker, B. W., L. Lothstein, C. L. Baker, and W. M. LeStourgeon. 1980. The release of 40S hnRNP particles by brief digestion of HeLa nuclei with micrococcal nuclease. *Nucleic Acid Res.* 8:3639–3657.
4. Samarina, O. P., E. M. Lukanidin, J. Molnar, and G. P. Georgiev. 1968. Structural organization of nuclear complexes containing DNA-like RNA. *J. Mol. Biol.* 33:251–263.
5. Beyer, A. L., M. E. Christensen, B. W. Walker, and W. M. LeStourgeon. 1977. Identification and characterization of the packaging proteins of core 40S hnRNP particles. *Cell.* 11:127–138.
6. Martin, T. E., and C. S. Okamura. 1981. Immunocytochemistry of nuclear hnRNP complexes. *In* The Cell Nucleus, Vol. 9. H. Busch, editor. Academic Press, Inc., New York. 119–144.
7. Sommerville, J. 1981. Immunolocalization and structural organization of nascent RNP. *In* The Cell Nucleus, Vol. 8. H. Busch, editor. Academic Press, Inc., New York. 1–57.
8. Martin, T. E., P. B. Billings, A. Levy, S. Ozarslan, T. Quinlan, H. Swift, and L. Urbas. 1974. Some properties of RNA:protein complexes from the nucleus of eukaryotic cells. *Cold Spring Harbor Symp. Quant. Biol.* 38:921–932.
9. LeStourgeon, W. M., A. E. Beyer, M. E. Christensen, B. W. Walker, S. M. Pourpore, and L. P. Daniels. 1978. The packaging proteins of core hnRNP particles and the maintenance of proliferative cell states. *Cold Spring Harbor Symp. Quant. Biol.* 42:885–897.
10. Economidis, I. V., and T. Pederson. 1983. Structure of nuclear ribonucleoprotein: heterogeneous nuclear RNA is complexed with a major sextet of proteins *in vivo*. *Proc. Natl. Acad. Sci. USA.* 80:1599–1602.
11. Karn, J., G. Vidali, L. C. Boffa, and V. G. Allfrey. 1977. Characterization of the nonhistone nuclear proteins associated with rapidly labeled heterogeneous nuclear RNA. *J. Biol. Chem.* 252:7307–7322.
12. Wilk, H-E., G. Angeli, and K. P. Schafer. 1983. *In vitro* reconstitution of 35S ribonucleoprotein complexes. *Biochemistry.* 22:4592–4600.
13. Tsanev, R. G., and L. P. Djoudjurov. 1982. Ultrastructure of Free ribonucleoprotein complexes in spread mammalian nuclei. *J. Cell Biol.* 94:662–666.
14. Beyer, A. L., O. L. Miller, and S. L. McKnight. 1980. Ribonucleoprotein structure in nascent hnRNA is non-random and sequence-dependent. *Cell.* 20:75–84.
15. Beyer, A. L., A. H. Bouton, and O. L. Miller, Jr. 1981. Correlation of hnRNP structure and nascent transcript cleavage. *Cell.* 26:155–165.
16. Knowler, J. T. 1983. An assessment of the evidence for the role of ribonucleoprotein particles in the maturation of eukaryote mRNA. *Int. Rev. Cytol.* 84:103–153.
17. Pederson, T. 1983. Nuclear RNA-protein interactions and messenger RNA processing. *J. Cell Biol.* 97:1321–1326.
18. Samarina, O. P., and A. A. Krichevskaya. 1981. Nuclear 30S RNP particles. *In* The Cell Nucleus, Vol. 9. H. Busch, editor. Academic Press, Inc., New York. 1–48.
19. Mayrand, S., and T. Pederson. 1981. Nuclear ribonucleoprotein particles probed in living cells. *Proc. Natl. Acad. Sci. USA.* 78:2208–2212.
20. van Eekelen, C. A., T. Riemen, and W. J. van Venrooij. 1981. Specificity in the interaction of hnRNA and mRNA with proteins as revealed by in vivo cross linking. *FEBS Fed. Eur. Biochem. Soc. Lett.* 130:223–226.
21. Marczinovits, I., and J. Molnar. 1982. Ultraviolet light-induced crosslinking of hnRNA to informofer proteins *in vitro*. *Mol. Biol. Rep.* 8:111–116.
22. Steitz, J. A., and R. Kamen. 1981. Arrangement of 30S heterogeneous nuclear ribonucleoprotein on polyoma virus late nuclear transcripts. *Mol. Cell Biol.* 1:21–34.
23. Stevenin, J., H. Gallinaro-Matringe, R. Gattoni, and M. Jacob. 1977. Complexity of the structure of particles containing heterogeneous nuclear RNA as demonstrated by ribonuclease treatment. *Eur. J. Biochem.* 74:589–602.
24. Stevenin, J., R. Gattoni, G. Divilliers, and M. Jacob. 1979. Rearrangements in the course of ribonuclease hydrolysis of pre-messenger ribonucleoproteins. *Eur. J. Biochem.* 95:593–606.
25. Kloetzel, P. M., R. M. Johnson, and J. Sommerville. 1982. Interaction of the hnRNA of amphibian oocytes with fibril forming protein. *Eur. J. Biochem.* 127:301–308.
26. LeStourgeon, W. M., and A. L. Beyer. 1977. The rapid isolation, high resolution electrophoretic characterization, and purification of nuclear proteins. *In* Methods in Chromosomal Protein Research. G. Stein, editor. Academic Press, Inc., New York. 387–406.
27. Wang, K., and F. M. Richards. 1974. The behavior of cleavable crosslinking reagents based on the disulfide groups. *Isr. J. Chem.* 12:375–389.
28. Wang, K., and F. M. Richards. 1974. An approach to nearest neighbor analysis of membrane proteins. *J. Biol. Chem.* 249:8005–8018.
29. Lothstein, L. 1983. Investigation of the arrangement of proteins and RNA in heterogeneous nuclear ribonucleoprotein particles from HeLa cells. Doctoral Thesis, Vanderbilt University.
30. Spitnik-Elson, P., and A. Breiman. 1971. The effect of trypsin on 30S and 50S ribosomal subunits of E. coli. *Biochem. Biophys. Acta.* 254:457–467.
31. Loeb, J. E., E. Ritz, C. Creuzet, and J. Jami. 1976. Comparison of chromosomal proteins of mouse primitive teratocarcinoma, liver, and L cells. *Exp. Cell Res.* 103:450–453.
32. Peters, K. E., and D. E. Commings. 1980. Two-dimensional gel electrophoresis of rat liver nuclear washes, nuclear matrix, and hnRNP proteins. *J. Cell Biol.* 86:135–155.
33. Holcomb, E. R., and D. L. Friedman. 1984. Phosphorylation of the C-Proteins of HeLa cell hnRNP particles: involvement of a casein kinase II-type enzyme. *J. Biol. Chem.* 259:31–40.
34. Dreyfuss, G., Y. D. Choi, and S. A. Adam. 1984. Characterization of heterogeneous nuclear RNA-Protein complexes in vivo with monoclonal antibodies. *Mol. Cell Biol.* 4:1104–1114.
35. Dubochet, J., and E. Kellenberger. 1972. Selective adsorption of particles to the supporting film and its consequence on particle counts in electron microscopy. *Microsc. Acta.* 72:119–130.
36. Stevenin, J., and M. Jacob. 1979. Structure of pre-mRNP, models and pitfalls. *Mol. Biol. Rep.* 5:29–35.
37. Spirin, A. S. 1969. Informosomes. *Eur. J. Biochem.* 10:20–35.
38. Lowry, O. H., N. J. Rosebrough, A. L. Farr, and R. J. Randall. 1951. Protein measurement with the Folin phenol reagent. *J. Biol. Chem.* 193:265–275.
39. Goldenberg, D. P., P. B. Berget, and J. King. 1982. Maturation of the tail spike endorhamnosidase of Salmonella phage P22. *J. Biol. Chem.* 257:7864–7871.
40. Choi, Y. D., and G. Dreyfuss. Isolation of the hnRNA-ribonucleoprotein complex (hnRNP): a unique supramolecular assembly. 1984 *Proc. Natl. Acad. Sci. USA.* 81:7471–7475.